

Magnetic susceptibility of antiferromagnetic chromium

C. A. Moyer and S. Arajs

Department of Physics, Clarkson College of Technology, Potsdam, New York 13676

L. Hedman

Department of Solid State Physics, Royal Institute of Technology, Stockholm, Sweden

(Received 1 March 1976)

The static magnetic susceptibility of pure chromium $\chi(T)$ has been measured over the temperature range from 4.3 to 340 K. The experimental results are compared with a theory based on the Fedders-Martin model of an antiferromagnet generalized to include bands of arbitrary shape. Fair agreement between theory and experiment is found for $\chi(T)$ from the Néel temperature ~ 312 K down to about 130 K. At 90 K the actual susceptibility passes through a minimum, then rises again with decreasing temperature. Neither the minimum nor the observed increase at low temperature are predicted by the theoretical model.

INTRODUCTION

Metallic chromium exhibits a very unique antiferromagnetic structure below 312 K. This structure results from conduction electrons condensing into a state of static spin-density waves^{1,2} whose wave vectors are slightly incommensurate with the reciprocal lattice. These waves are transverse linearly polarized (the wave vector of the spin-density wave is perpendicular to the spin polarization vector) between about 123 and 312 K, and longitudinally polarized below 123 K. Such an itinerant electron antiferromagnetism is a truly rare phenomenon and can exist only in specific electronic structures over a limited range of electron concentrations.³⁻⁵ Therefore different physical properties of binary chromium alloys have received considerable attention in the past from both experimental and, to some extent, theoretical viewpoints. In spite of some general progress toward a better understanding of this unique antiferromagnetic state, numerous and fundamentally important questions still remain completely or partially unanswered. One such incompletely understood area is the static magnetic behavior of itinerant binary chromium systems. We report here our recent experimental results for the static magnetic susceptibility versus temperature of pure antiferromagnetic chromium, and compare them with theoretical predictions based on a generalized Fedders-Martin model of the antiferromagnetic state.

THEORETICAL CONSIDERATIONS

Owing to its itinerant antiferromagnetism, chromium exhibits an anomalous spin susceptibility below the magnetic ordering (Néel) temperature T_N . The gross features of the χ vs T curve can be understood from elementary arguments based on a two-sublattice model of atomic spins.

A strong anisotropy is found according to the orientation of the external field \vec{H} relative to the direction of magnetization $\vec{\mu}$ of the two sublattices. In the perpendicular orientation the susceptibility χ_{\perp} is nearly independent of temperature; the polarization of the sublattices normal to the applied field exerts only a feeble opposition to their magnetization being slightly turned in the field direction. On the other hand, χ_{\parallel} goes to zero at zero temperature because the internal field is so strong that it prevents any spins in the opposing sublattice from turning over. The parallel susceptibility increases smoothly with temperature until the anisotropy disappears at T_N .

In a macroscopic sample crystal orientations are randomized, so that the measured susceptibility χ should be

$$\chi(T) = \frac{1}{3}\chi_{\parallel} + \frac{2}{3}\chi_{\perp}, \quad (1)$$

and $\chi(0)$ should have the average value of $\frac{2}{3}\chi_{\perp}$. These predictions are borne out qualitatively by the chromium susceptibility data, despite the fact that the antiferromagnetism of chromium is attributed to itinerant conduction-band electrons.

The first susceptibility studies pertinent to itinerant antiferromagnets like chromium were undertaken by Fedders and Martin⁵ (FM). Following Lomer,³ FM proposed a two-band model for chromium in which antiferromagnetism results from the nesting of electron and hole pieces of the Fermi surface. The antiferromagnetic state thus stabilized below T_N is a spin-density wave having a net conduction-electron spin polarization $\vec{P}(\vec{r})$ at every point, whose amplitude at equivalent points in the crystal lattice is modulated sinusoidally with a period determined by the Fermi-surface geometry and generally incommensurate with the lattice. The direction of spin variation defines the axis \vec{q} of the spin-density wave with wave number $|\vec{q}|$. The FM state is

transverse linearly polarized, corresponding to a fixed direction of polarization \vec{P} which is everywhere perpendicular to \vec{q} .

On the itinerant picture there is a gap energy which keeps the spin antiferromagnetic and depresses the susceptibility χ below T_N . The gap energy $g(T)$ in the FM model is given implicitly as the solution of

$$1 = \frac{\gamma^2 v(0)}{2(2\pi)^3} \int d^3K \frac{1}{E} \tanh\left(\frac{\beta E}{2}\right). \quad (2)$$

Here $v(0)$ is the strength of the (screened) electron-electron repulsion, γ is a suitably averaged matrix element of v , $\beta = 1/K_B T$, and

$$E = [\epsilon^2(K) + g^2(T)]^{1/2}, \quad (3)$$

where $\epsilon(K)$ is the one-electron energy measured from the Fermi surface. T_N is fixed by the condition that the gap energy vanish at the transition temperature.

The parallel and perpendicular spin susceptibilities are calculated in the FM theory as

$$\chi_{\parallel}(T) = \frac{2\mu_B^2}{(2\pi)^3} \int d^3K \frac{\partial}{\partial E} \tanh\left(\frac{\beta E}{2}\right), \quad (4)$$

$$\chi_{\perp}(T) = \frac{2\mu_B^2}{(2\pi)^3} \int d^3K \left[\left(\frac{g^2}{E^3}\right) \tanh\left(\frac{\beta E}{2}\right) - \frac{g^2}{E^2} \frac{\partial}{\partial E} \tanh\left(\frac{\beta E}{2}\right) \right] + \chi_{\parallel}(T), \quad (5)$$

where μ_B is the Bohr magneton.

We have applied these equations to the study of the static magnetic susceptibility in pure chromium. The band structure $\epsilon(\vec{K})$ need not be specified further, since the whole theory is fixed by the density of states and its curvature at the Fermi energy. This generalizes the original work of Fedders and Martin, where a linear dependence of ϵ on K was assumed in the context of spherical bands.

Gap energy $g(T)$. By introducing the density of states $\rho(\epsilon)$, we can write the integral in Eq. (2) as

$$\int d^3K - \int_{\epsilon_1}^{\epsilon_2} d\epsilon \frac{\rho(\epsilon)}{E} \left\{ 1 + \left[\tanh\left(\frac{\beta E}{2}\right) - 1 \right] \right\}, \quad (6)$$

where $\epsilon_{1,2}$ are the band limits measured from the Fermi energy. The first term is

$$\begin{aligned} \int_{\epsilon_1}^{\epsilon_2} d\epsilon \frac{\rho(\epsilon)}{E} &= 2\rho(0) \ln \left| \frac{2\epsilon_1}{g} \right| + \mathcal{P} \int_{\epsilon_1}^{\epsilon_2} \frac{d\epsilon}{\epsilon} \rho(\epsilon) \\ &\quad - \frac{\rho''(0)}{2} g^2 \ln \left| \frac{2\epsilon_1}{g} \right| \\ &\quad + O(g/\epsilon_1)^2, \end{aligned} \quad (7)$$

where \mathcal{P} denotes Cauchy principal value. The dominant contribution to the second term comes from the region around the Fermi energy $\epsilon = 0$. Representing ρ there by its Taylor series

$$\rho(\epsilon) \approx \rho(0) + \rho'(0)\epsilon + \rho''(0)\left(\frac{1}{2}\epsilon^2\right) \quad (8)$$

and extending the integration limits to infinity gives

$$\begin{aligned} \int_{\epsilon_1}^{\epsilon_2} d\epsilon \frac{\rho(\epsilon)}{E} \left(\tanh\left(\frac{\beta E}{2}\right) - 1 \right) \\ \approx -4\rho(0)\bar{K}_0(\beta g) + \rho''(0)g^2 [\bar{K}_0(\beta g) - \bar{K}_2(\beta g)], \end{aligned} \quad (9)$$

where $\bar{K}_\nu(z)$ are functions (defined in the appendix) which reduce to the modified Bessel functions $K_\nu(z)$ in the limit of large z .

$g(T)$ is given in terms of g_0 , the zero-temperature gap, by

$$\int_{\epsilon_1}^{\epsilon_2} d\epsilon \frac{\rho(\epsilon)}{E} \Big|_{\epsilon}^{\epsilon_0} = \int_{\epsilon_1}^{\epsilon_2} d\epsilon \frac{\rho(\epsilon)}{E} \left[\tanh\left(\frac{\beta E}{2}\right) - 1 \right]. \quad (10)$$

At the Néel temperature T_N g vanishes identically and Eqs. (7), (9), and (10) give

$$\begin{aligned} g_0 &= \left\{ \frac{4\pi e^{-\psi(1/2)}}{\beta_N} \right\} \\ &\times \exp \left[\frac{\rho''(0)g_0^2}{4\rho(0)} \left(\frac{\pi^2}{3\beta_N^2 g_0^2} - \ln \left| \frac{2\epsilon_1}{g_0} \right| \right) \right], \end{aligned} \quad (11)$$

where ψ is the digamma function. The quantity in large curly brackets is the simple FM result for a linear band structure; with $T_N \approx 312$ K the predicted gap is $g_0 \approx 0.044$ eV. The correction factor may reduce this value appreciably. Indeed, the chromium susceptibility data suggest $g_0 \approx 0.028$ eV.

Combining Eqs. (7)–(11) yields an implicit equation for $g(T)$:

$$\begin{aligned} \left(1 - \frac{\rho''(0)g^2}{4\rho(0)} \right) \ln \left(\frac{g}{g_0} \right) \\ - \left(\psi\left(\frac{1}{2}\right) + \ln \frac{4\pi}{\beta_N g_0} + \frac{\pi^2 \rho''(0)}{12\rho(0)\beta_N^2} \right) \left(1 - \frac{g^2}{g_0^2} \right) \\ \approx -2\bar{K}_0(\beta g) + \frac{\rho''(0)g^2}{2\rho(0)} [\bar{K}_0(\beta g) - \bar{K}_2(\beta g)]. \end{aligned} \quad (12)$$

Near T_N $g(T)$ vanishes as $(T_N - T)^{1/2}$, while the curve is remarkably flat at low temperature. Figure 1 shows $g(T)$ calculated numerically from Eq. (12) for parameters giving the best fit to the chromium susceptibility data.

Parallel susceptibility χ_{\parallel} . In terms of the density of states $\rho(\epsilon)$ Eq. (4) becomes

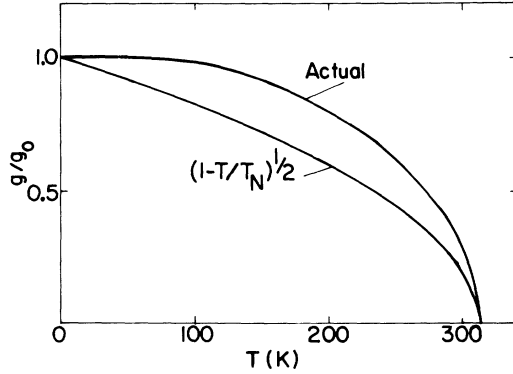


FIG. 1. Temperature dependence of the antiferromagnetic gap energy $g(T)$ computed from the generalized Fedders-Martin model. The familiar BCS-like gap is shown for comparison.

$$\chi_{\parallel} = \frac{2\mu_B^2}{(2\pi)^3} \frac{\beta}{2} \int_{\epsilon_1}^{\epsilon_2} d\epsilon \rho(\epsilon) \operatorname{sech}^2\left(\frac{\beta E}{2}\right). \quad (13)$$

Again the main contribution to the integral comes from the Fermi energy. Proceeding as before we obtain

$$\chi_{\parallel} \approx \chi_0 \left(-2\beta g \bar{K}'_0(\beta g) + \frac{\rho''(0)g^2}{2\rho(0)} \beta g [\bar{K}'_0(\beta g) - \bar{K}'_2(\beta g)] \right). \quad (14)$$

Here a prime denotes differentiation with respect to the argument and

$$\chi_0 = [2\mu_B^2 / (2\pi)^3] 2\rho(0) \quad (15)$$

is the familiar Pauli susceptibility. At T_N

$$\chi_{\parallel} = \chi_0 \left[1 + \pi^2 \rho''(0) / 6\rho(0) \beta_N^2 \right], \quad (16)$$

which differs from χ_0 . The discrepancy may be traced to the additional band-structure details contained in $\rho''(0)$. As expected, χ_{\parallel} decreases rapidly with temperature, vanishing exponentially as T approaches zero:

$$\chi_{\parallel} \sim \chi_0 (2\pi\beta g)^{1/2} e^{-\beta g}. \quad (17)$$

Perpendicular susceptibility χ_{\perp} . In place of Eq. (5), a more convenient expression for calculating χ_{\perp} may be obtained by differentiating the gap equation (2) to get

$$\chi_{\perp} = \left(1 + \frac{g}{\beta} \frac{d\beta}{dg} \right) \chi_{\parallel}. \quad (18)$$

With Eqs. (12) and (14), this yields, after some manipulation,

$$\chi_{\perp} \approx \chi_0 \left[1 + 2\psi\left(\frac{1}{2}\right) + 2 \ln\left(\frac{4\pi}{\beta_N g}\right) + \frac{\rho''(0)}{4\rho(0)} \left(\frac{2\pi^2}{3\beta_N^2} - g^2 \right) - 4\bar{K}'_0(\beta g) \right]. \quad (19)$$

χ_{\perp} coincides with χ_{\parallel} at T_N , but actually increases with decreasing T , slowly reaching the zero-temperature limit

$$\chi_{\perp}(0) = \chi_0 \left[1 + 2\psi\left(\frac{1}{2}\right) + 2 \ln\left(\frac{4\pi}{\beta_N g_0}\right) + \frac{\rho''(0)}{4\rho(0)} \left(\frac{2\pi^2}{3\beta_N^2} - g_0^2 \right) \right] \quad (20a)$$

$$= \chi_0 \left[1 + \frac{\rho''(0)}{2\rho(0)} g_0^2 \left(\ln \left| \frac{2\epsilon_1}{g_0} \right| - \frac{1}{2} \right) \right], \quad (20b)$$

where Eq. (20b) follows from Eq. (11). Figure 2 shows the parallel and perpendicular contributions to the susceptibility below T_N calculated numerically from Eqs. (14) and (19) using parameters giving the best fit to the chromium susceptibility data.

EXPERIMENTAL CONSIDERATIONS

The chromium sample, whose magnetic properties are reported in this paper, was prepared from an arc-melted ingot using chromium (Iochrome iodide crystals) obtained from Chromalloy Corporation. The analysis of the impurities found in this material has been given previously.⁶ The arc melting of this material was done by means of facilities and techniques described elsewhere.⁷ The magnetic susceptibility data shown in Fig. 3 (dotted curve) were obtained using an annealed polycrystalline sample (at 1000 °C for about 8 h followed by slow cooling at room temperature). The mass of this specimen was about 0.3 g. The magnetic susceptibility measurements were made, starting at 4.2 K, with increasing

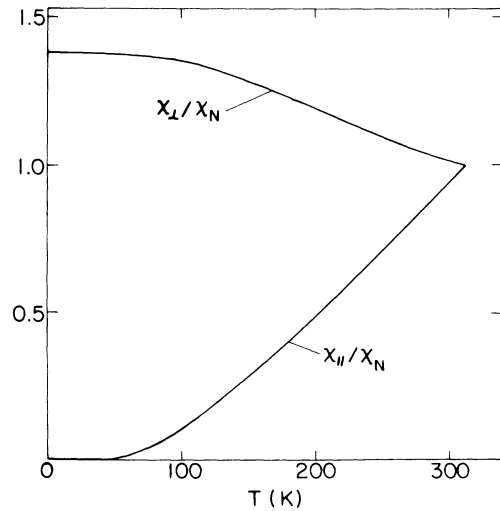


FIG. 2. Parallel and perpendicular components of susceptibility computed from the generalized Fedders-Martin model of an antiferromagnet.

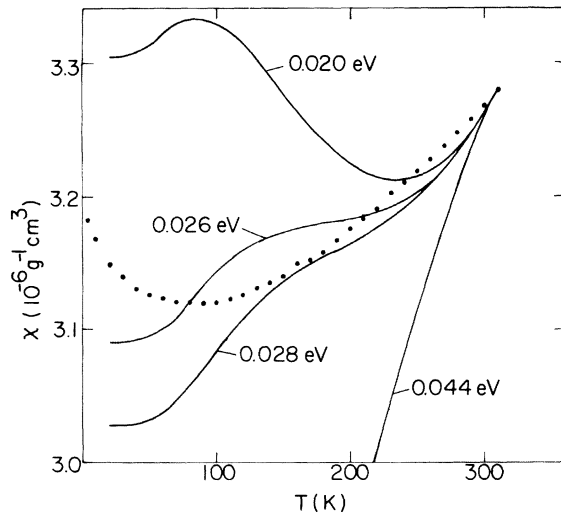


FIG. 3. Experimental results for the susceptibility of antiferromagnetic chromium. Solid curves are theoretical predictions of the generalized Fedders-Martin model for several values of the antiferromagnetic gap energy g_0 .

temperatures using the equipment based on the Faraday method described briefly in a previous paper.⁸

RESULTS AND DISCUSSION

Figure 3 compares the theoretical prediction for $\chi = \frac{1}{3}\chi_{\parallel} + \frac{2}{3}\chi_{\perp}$ from Eqs. (14) and (19) with the experimental results on an annealed polycrystalline sample over the range 4–340 K. The Néel temperature was determined to be 311.8 ± 0.2 K.

The experimental χ vs T curve clearly shows a broad minimum at about 90 K, followed by a gradual increase in χ with decreasing temperatures. A similar behavior in pure chromium has been noted before.^{9–11} It is tempting to think that such a behavior results from magnetic impurities possessing localized magnetic moments. However, we believe that the increase in χ at low temperatures is an intrinsic property of chromium for the following reasons: First, the content of iron in our chromium sample is only about 10 ppm, an amount much too small to cause the observed effect. Furthermore, the level of cobalt and manganese is even lower, about 1 ppm or less. Second, some limited experimental studies indicate that the minimum mentioned above remains approximately unchanged when, for example, titanium is dissolved in chromium,¹¹ but gradually disappears when silicon is added to the chromium matrix.¹²

Finally, it should be remarked that pure chromium undergoes a very small step-type decrease¹³

in χ with decreasing temperatures at the spin-flip transition (123 K). Because of its small size, this anomaly is not observable in the χ vs T plot shown in Fig. 3.

In constructing the theoretical curves the density of states at the Fermi energy $\rho(0)$ and its curvature $\rho''(0)$ were chosen to reproduce the observed value and slope of the susceptibility at the Néel temperature. With this procedure the best fit to the data down to about 130 K was obtained for $g_0 \approx 0.028$ eV. Other estimates of the gap energy obtained by optical methods give somewhat higher values.^{14,15} The susceptibility predictions are very sensitive to the gap energy, as shown again by Fig. 3. $g_0 = 0.044$ eV is the gap energy in the simple FM model obtained by taking $\rho''(0) = 0$ in Eq. (11). We conclude that the density-of-states curvature at the Fermi energy is significant in harmonizing theory with experiment for the susceptibility in the high-temperature regime below T_N . The actual curvature deduced from the data is

$$[\rho''(0)/2\rho(0)]g_0^2 \approx 0.403.$$

For no choice of g_0 was it possible to fit the observed results below about 120 K. In particular, the broad temperature minimum in the chromium susceptibility around 90 K defies explanation within the present framework. Apparently, some important mechanism has been overlooked. One possibility concerns the samples themselves, which are polycrystalline. Thus a mixture of spin-density wave vectors \vec{q} of varying orientation is represented, and comparison of theory with experiment presupposes this distribution to be random. Any mechanism invalidating the randomness supposition would have a significant effect, particularly at lower temperatures, where one expects strong anisotropy in χ . To check this hypothesis, susceptibility measurements were repeated on chromium samples which had been cold worked. Cold working ensures random \vec{q} orientations, thus eliminating any doubts concerning directional averaging. No significant deviations from the original sample data were found. For the purpose of clarity, these measurements are not included in Fig. 3. The small effects of cold work on χ at T_N and at the spin-flip transition as a function of warming and cooling rates will be reported in a separate publication. The cold-worked samples did reveal, however, an enhancement in the anomaly at the spin-flip transition. In general, spin flip appears to lower the susceptibility, but not nearly enough to account for the observed minimum or the rise in χ at low temperatures.

Other contributory mechanisms overlooked in

the theory include the susceptibility of electrons in other (nonmagnetic) chromium bands and the influence of collective modes (spin wave excitations). Estimates by Windsor¹⁶ and Gupta and Sinha¹⁷ indicate the other band contributions are appreciable at the magnetic ordering temperature, but the temperature dependence is an unknown quantity. Nevertheless, other band contributions would certainly help to bring the theory into better agreement with the high-temperature data below T_N .

At low temperatures the collective modes are expected to dominate the response. At zero temperature the FM model antiferromagnet does exhibit a collective mode with a soundlike dispersion law at long wavelengths. Failure of the present theory to account satisfactorily for the low-temperature results is likely due to the presence of these collective excitations, whose influence on $\chi(T)$ has not yet been assessed.

ACKNOWLEDGMENTS

The authors are grateful to the U. S. National Science Foundation (S.A.), the Research Corporation (C.A.M.), and Swedish Statens Naturvetenskapliga Forskningsråd (L.H.) for the financial support of this work. Helpful discussions with Professor K. V. Rao and Professor H. U. Åström, also are greatly appreciated.

APPENDIX

The functions \tilde{K}_ν are defined by

$$\tilde{K}_\nu(z) = \int_0^\infty \frac{dt}{e^z \cosh t + 1} \cosh \nu t. \quad (\text{A1})$$

The relationship to Bessel functions $K_\nu(z)$ is readily established by expanding the denominator of the integrand according to the binomial theorem and using the integral representation of K_ν ,

$$\tilde{K}_\nu(z) = \sum_1^\infty (-1)^{n+1} K_\nu(nz). \quad (\text{A2})$$

Equation (A2) is also useful for computation when z is large.

Functional equations for \tilde{K}_ν may be obtained directly from the Bessel-function recursion relations. In particular, from

$$\frac{d}{dz} [z^2 K_2(z)] = -z^2 K_1(z) = z^2 \frac{d}{dz} K_0(z) \quad (\text{A3})$$

we deduce

$$\frac{d}{dz} [z^2 \tilde{K}_2(z)] = z^2 \frac{d}{dz} \tilde{K}_0(z), \quad (\text{A4})$$

which may be integrated to give

$$z^2 \tilde{K}_2(z) = \lim_{z \rightarrow 0} z^2 \tilde{K}_2(z) + \int_0^z z^2 \frac{d}{dz} \tilde{K}_0(z) dz. \quad (\text{A5})$$

Letting $z \rightarrow \infty$ in Eq. (A5) allows evaluation of the limit as

$$\lim_{z \rightarrow 0} z^2 \tilde{K}_2(z) = 2 \int_0^\infty z \tilde{K}_0(z) dz = 2 \int_0^\infty \frac{\omega d\omega}{e^\omega + 1} = \frac{\pi^2}{6}, \quad (\text{A6})$$

where Eq. (A1) has been used for K_0 .

Representations useful when z is small derive from the interesting formula¹⁸

$$\tilde{K}_0(z) = \frac{1}{2} \ln \frac{4\pi}{z} - \frac{\gamma}{2} - \pi \sum_1^\infty \left([z^2 + (2n-1)^2 \pi^2]^{-1/2} - \frac{1}{2n\pi} \right), \quad (\text{A7})$$

where γ is Euler's constant. For $|z| < \pi$ the radical can be expanded as a power series in z to get

$$\tilde{K}_0(z) = \frac{1}{2} \ln \frac{4\pi}{z} + \frac{1}{2} \psi\left(\frac{1}{2}\right) - (1/32\pi^2) \psi''\left(\frac{1}{2}\right) z^2 + O(z^4), \quad (\text{A8})$$

where ψ is the digamma function. The corresponding formula for $\tilde{K}_2(z)$ then follows directly from Eqs. (A5) and (A6):

$$\tilde{K}_2(z) = \pi^2/6z^2 - \frac{1}{4} - (1/64\pi^2) \psi''\left(\frac{1}{2}\right) z^2 + O(z^4).$$

¹A. W. Overhauser, Phys. Rev. **128**, 1437 (1962).

²A. Arrott, in *Magnetism: A Treatise on Modern Theory and Materials*, edited by G. T. Rado and H. Suhl (Academic, New York, 1966), p. 296.

³W. M. Lomer, Proc. Phys. Soc. Lond. **80**, 489 (1962).

⁴D. Penn, Phys. Rev. **142**, 350 (1966).

⁵P. A. Fedders and P. C. Martin, Phys. Rev. **143**, 245 (1966).

⁶S. Arajs and G. R. Dunmyre, J. Appl. Phys. **36**, 3555 (1965).

⁷S. Arajs and G. P. Wray, J. Phys. E **2**, 518 (1969).

⁸L. Hedman, K. Svensson, K. V. Rao, and S. Arajs, Phys. Lett. A **45**, 175 (1973).

⁹R. Lingelbach, Z. Phys. Chem. (Leipz.) **14**, 1 (1958).

¹⁰Y. Ishikawa, R. Tournier, and J. Filippi, J. Phys. Chem. Solids **26**, 1727 (1965).

¹¹C. H. Chiu, M.H. Jericho, and R. M. March, Can. J. Phys. **49**, 3010 (1971).

¹²S. Arajs, K. V. Rao, L. Hedman, and H. U. Åström, in *Low Temperature Physics-LT14*, edited by M. Krusius and M. Vuorio (North-Holland, Amsterdam, 1975), Vol. 3, p. 231.

- ¹³L. Hedman, K. Svensson, K. V. Rao, S. Arajs, and H. U. Åström, *J. Low Temp. Phys.* 14, 545 (1974).
- ¹⁴A. S. Barker, Jr. and J. A. Ditzenberger, *Phys. Rev. B* 1, 4378 (1970).
- ¹⁵L. W. Bos, D. W. Lynch, and J. L. Stanford, *Phys. Lett. A* 30, 17 (1969).
- ¹⁶C. G. Windsor, *J. Phys. F* 2, 742 (1972).
- ¹⁷R. P. Gupta and S. K. Sinha, *Phys. Rev. B* 3, 2401 (1971).
- ¹⁸I. M. Ryshik and I. S. Gradstein, in *Tables of Series, Products, and Integrals* (VEB Deutscher Verlag der Wissenschaften, Berlin, 1957), p. 335.